Metal–Organic Frameworks

DOI: 10.1002/anie.200704702

Metal–Organic Nanoporous Structures with Anisotropic Photoluminescence and Magnetic Properties and Their Use as Sensors**

Bogdan V. Harbuzaru, Avelino Corma, Fernando Rey, Pedro Atienzar, Jose L. Jordá, Hermenegildo García, Duarte Ananias, Luis D. Carlos, and João Rocha**

Dedicated to Professor Wolfgang Herrmann on the occasion of his 60th birthday

The field of multifunctional materials has seen very rapid progress since the discovery of structures with a variety of technologically useful properties such as nanoporosity,[1–3] luminescence, and magnetism for sensors,[4–6] lasers,[7,8] nonlinear optics,[9] displays,[10] and electroluminescent devices.[11] After these discoveries, one of the most appealing aims is to explore multifunctionality, especially in designed materials, which combine in the same crystal a set of well-defined properties for specific applications. Lanthanide-based porous metal–organic frameworks (Ln-MOFs)[12–17] are excellent candidates to create multifunctional materials for sensors, provided that their photoluminescence and emission lifetimes are not influenced at ambient conditions by the presence of water.[5,18–20] Existing Ln-MOF materials are thermally stable in air only up to approximately 673 K,[5,18,21] while pore diameters are too small to allow the diffusion of molecules of interest.[21,22] These properties preclude their use in luminescence sensors working in the presence of moisture at ambient temperature.

MOFs that combine magnetic and anisotropic properties with high emission quantum yields under ambient conditions will open new possibilities for low-cost sensors.[23] Herein, we have synthesized, by rational design, novel crystalline MOFs containing rare-earth ions that combine hydrophobicity, high adsorption capacity, high thermal resistance, anisotropic photoluminescence, and magnetic properties. These materials preserve their photoluminescence properties in the presence of water and show excellent sensor capabilities.

For achieving the above properties, we have chosen an organic spacer that fulfils the following requirements: high hydrophobicity, antenna effect, strong interaction with the metal center, and at least two coordination centers in order to obtain microporous 3D structures. High hydrophobicity was attained with ultrahydrophobic ligands, such as multiaromatic and C(sp^3) fluorinated spacers. The antenna effect can be present in a spacer with aromatic or multiaromatic groups. Moreover, rare-earth ions have high affinity for oxygen-containing molecules, for example those with carboxy groups, which produce robust framework architectures.[24] One spacer that fulfills the above requirements and that can be adequate to synthesize MOFs[25–27] is 4,4′-(hexafluoroisopropylidene)-bis(benzoic acid) (HFIPBB).

Herein, under appropriate synthesis conditions and in the presence of HFIPBB, new Ln^{3+}-based materials ITQMOF-1 and ITQMOF-2 (ITQMOF = Instituto de Tecnologia Quimica Metal Organic Framework), with similar properties but different crystallographic structures, have been obtained. To obtain the desired properties (luminescence and magnetism), different samples have been prepared with all the Ln elements except for the radioactive promethium. For mixed Ln^{3+} samples, their molar composition (%) is given in parenthesis.

The ITQMOF-1 material was obtained by reacting the HFIPBB ligand with the corresponding Ln^{3+} salt or oxide at 423 K in an appropriate solvent (see the Supporting Information). The formula obtained by chemical and elemental analyses is $[Ln_2(C_{17}H_8F_6O_4)_3]$ for the solvent-free material. The ITQMOF-1 crystals[28] exhibit strong twinning, which prevents structure elucidation by single crystal diffraction, even using synchrotron radiation.

Large acicular crystals of ITQMOF-2 (Figure 1a) were obtained as a secondary phase from the synthesis of ITQMOF-1. The structure of ITQMOF-2-Eu was determined from single crystal diffraction data[28] collected at beamline BM16 at ESRF. The structure was solved using SHELXS-97[29] and refined with SHELXL-97.[30] The structure consists of parallel, zigzagging columns of alternating nona- and octa-coordinated Eu^{3+} ions in the direction of the *a* axis (Figure 1b). In a given column, the Eu^{3+} ions are connected through the oxygen atoms of the same carboxy groups of the

[*] Dr. B. V. Harbuzaru, Prof. Dr. A. Corma, Dr. F. Rey, Dr. P. Atienzar, Dr. J. L. Jordá, Prof. Dr. H. García
Instituto de Tecnología Química, (UPV-CSIC)
Universidad Politécnica de Valencia
Avda. de los Naranjos s/n, 46022 Valencia (Spain)
Fax: (+34) 96-387-7809
E-mail: acorma@itq.upv.es
Dr. D. Ananias, Prof. Dr. L. D. Carlos, Prof. Dr. J. Rocha
Departments of Chemistry and Physics, CICECO
University of Aveiro
3810-193 Aveiro (Portugal)

[**] The authors thank Spanish CICYT for financial support (MAT2006-08039, MAT2006-14274-C02-01), and Beamline BM-16 at ESRF in Grenoble for beam time allocation. Also, the authors would like to thank the European Network of Excellence FAME. D.A., L.D.C., and J.R. thank FTC and FEDER. J.L.J. thanks I3 program of CSIC (200680|180) for partial financial support. We also thank F. Delgado-Trujillo for helpful discussions.

Supporting information for this article is available on the WWW under http://www.angewandte.org or from the author.

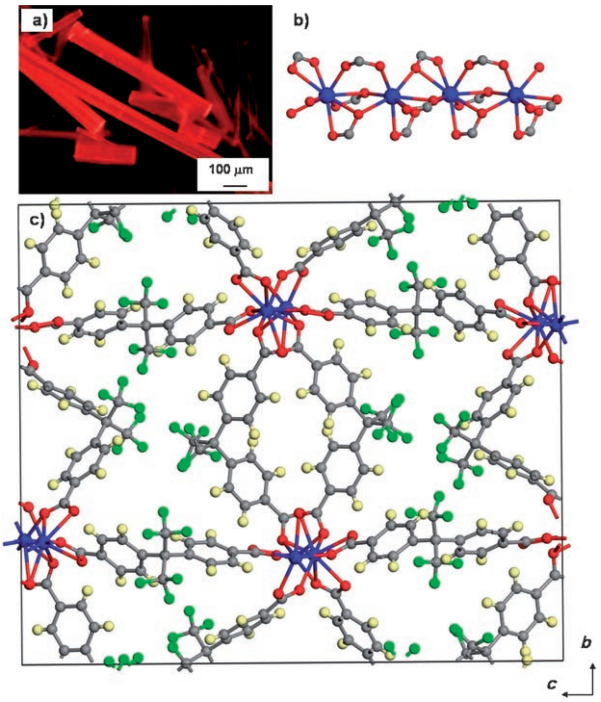

Figure 1. a) ITQMOF-2-Eu sample in UV light seen by optical microscopy. b) Chain with alternating eight- and nine-coordination for the Ln sites in ITQMOF-2. c) Structure of the ITQMOF-2 material (Eu blue, O red, C gray, F green, H yellow).

ligand, while neighboring columns are linked through the oxygen atoms of opposite carboxy groups of the ligand. The three symmetrically independent ligand molecules observed give rise to a microporous hydrophobic structure with both strongly hindered fluorinated channels and relatively free channels surrounded by the aromatic groups (Figure 1c).

Both materials, ITQMOF-1 and -2, are insoluble in water in hydrothermal conditions and in common organic solvents. The thermal stability of ITQMOF-1 and ITQMOF-2 materials is very high. Variable-temperature powder X-Ray diffraction and thermogravimetry show that the structure of ITQMOF-1 material is preserved up to above 673 K either in air or in helium and decomposes slowly around 723 K (see the Supporting Information, Figures S3 and S4).

The nitrogen adsorption isotherm of ITQMOF-1-Eu at 77 K, obtained after degassing the solvent-free sample at 483 K and 10^{-3} Pa for 4 h, gives a pore volume of 0.14 $cm^3 g^{-1}$ and a Brunauer–Emmett–Teller (BET) surface area of 207 $m^2 g^{-1}$ (see the Supporting Information, Figure S5). Most of the porosity is in the micropore region, as deduced from the t-plot analysis. However, the N_2 isotherm shows the presence of some porosity in the mesopore range.

For ITQMOF-1-Eu, ITQMOF-1-(5Eu-95Gd) (5 mol% Eu, 95 mol% Gd), and ITQMOF-1-(66Eu-34Gd) single crystals, the $^5D_0$ decay time has been measured monitoring the strongest $^7F_2$ Stark component (excitation wavelength 295 nm). The experimental data are well-described by single-exponential functions (see the Supporting Information, Figure S10), suggesting the presence of a unique Eu^{3+} crystallographic site.

The 10-K emission spectra of a ITQMOF-1-(5Eu-95Gd) single crystal excited at 295 nm and recorded for two different crystal orientations relative to the detector are shown in Figure 2a. The spectra exhibit a series of narrow lines

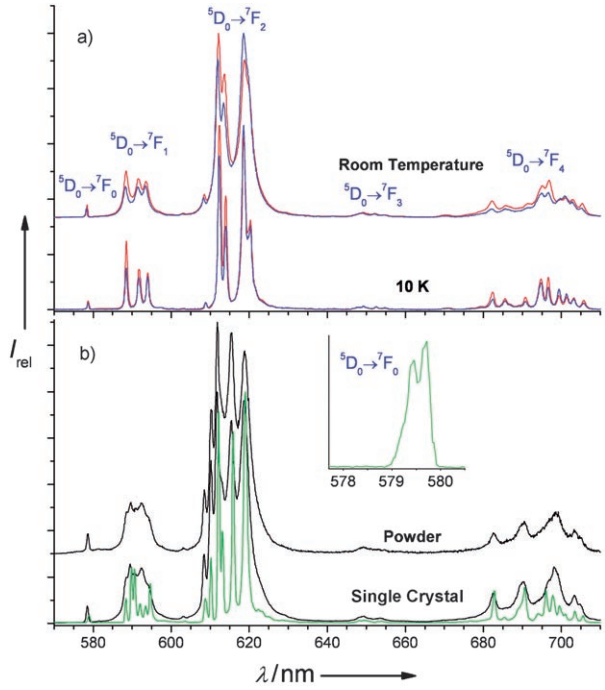

Figure 2. a) Emission spectra of a ITQMOF-1-(5Eu-95Gd) single crystal, recorded at room temperature and 10 K for two different orientations of the crystal relative to the detector (red line: vertical, blue line: horizontal). b) Emission spectra of ITQMOF-2-Eu powder and single crystal (oriented in the vertical position), recorded at room temperature (black line) and 10 K (green line). The inset shows an expansion of the $^5D_0 \rightarrow ^7F_0$ region at 10 K. In both cases, the excitation was performed at 290 nm.

ascribed to the Eu^{3+} $^5D_0 \rightarrow ^7F_{0-4}$ transitions. The $^5D_0 \rightarrow ^7F_{5,6}$ transitions are not experimentally detected. Both the local field splitting of the $^7F_{1,2,4}$ levels in, respectively, three, five, and nine Stark components and the presence of a single nondegenerated $^5D_0 \rightarrow ^7F_0$ line (17280.1 cm^{-1}, full width at half maximum (FWHM) of 13.5 cm^{-1}), suggest that the Eu^{3+} ions occupy a low-symmetry site without an inversion center (higher intensity for the $^5D_0 \rightarrow ^7F_2$ transition).

The 10-K and room-temperature emission spectra of a ITQMOF-2-Eu single crystal, excited at 290 nm, are shown in Figure 2b. The presence of two $^5D_0 \rightarrow ^7F_0$ lines and the local field splitting of the $^7F_1$ level into six Stark components indicates that the Eu^{3+} ions occupy two distinct, low-symmetry sites lacking an inversion center, in accord with the crystal structure. For the ITQMOF-2-Eu single crystals, the two $^5D_0$ lifetimes may be determined separately by monitoring the two first $^7F_1$ Stark components at 10 K. The decay curves are well-described by single-exponential functions, yielding lifetimes of 1.549 ± 0.012 ms and 1.595 ± 0.010 ms (excitation wavelength 290 nm).

The emission features of all Eu-containing ITQMOF-1 and 2 samples strongly depend on the orientation of the single crystals relative to the detector and incident beam, particularly for ITQMOF-1 materials (Figure 3a). The anisotropy effects on the emitted light are even more obvious when a polarizer is placed just before the detector (Figure 3b).

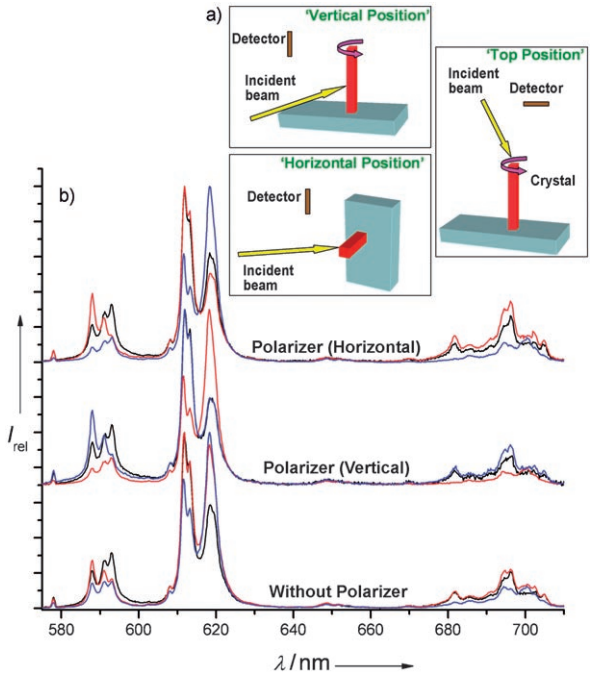

Figure 3. a) Experimental setup and single-crystal orientations studied. Note that the main difference between the "vertical" and "horizontal" positions is that in the former the plane of the detector and Xe light source are parallel to the crystal support, while in latter position the plane of the detector and the Xe lamp are perpendicular to the support. b) Room-temperature emission spectra of an ITQMOF-1-(5Eu-95Gd) single crystal, recorded using a polarizer just before the detector, for the three different crystal orientations (black line: top, red line: vertical, blue line: horizontal). The excitation was performed at 290 nm.

On the basis of the emission spectra and empirical radiative and nonradiative transition rates, the $^5D_0$ quantum efficiency[31–34] q has been determined for ITQMOF-1-Eu, ITQMOF-1-(5Eu-95Gd), and ITQMOF-1-(66Eu-34Gd) single crystals (Table 1).

Owing to the presence of two distinct Eu^{3+} sites, this parameter could not be estimated for the ITQMOF-2 sample. The ITQMOF-1-(5Eu-95Gd) sample is very efficient, with $q = 0.83$ (to our knowledge the highest $^5D_0$ quantum efficiency reported for solid-state Eu^{3+} compounds with organic ligands), exhibiting a good balance between absorption, energy-transfer, and emission rates. The relatively small contribution of the nonradiative paths for $^5D_0$ depopulation (less than 28% of the total transition rate) is worth mentioning. As the Eu^{3+} content increases from 5 to 100 mol%, the $^5D_0$ quantum efficiency decreases from 0.83 to 0.56, owing to the increase in nonradiative paths for $^5D_0$ depopulation (the radiative transition probability remains almost unchanged; Table 1). This result is ascribed to the activation of the energy transfer between the closely spaced Eu^{3+} ions.

The absolute emission quantum yield (η) has been measured for ITQMOF-1-(5Eu-95Gd) and ITQMOF-2-Eu single crystals (Table 1). The best material, ITQMOF-1-(5Eu-95Gd), presents the highest value (0.48, excitation wavelength of 290 nm) ever reported for Eu^{3+}-based MOFs, supporting the above-mentioned good balance between absorption, energy-transfer, and emission rates. An η value of 0.39 has been measured for ITQMOF-2-Eu.

The photoluminescence of ITQMOF-1 and 2 materials is not quenched by water. Indeed, the $^5D_0$ lifetime may be used to estimate the hydration number (n) in Eu^{3+} complexes.[19] For example, the $^5D_0$ lifetimes of ITQMOF-1-(5Eu-95Gd), measured before and after exposure to water vapor, are 1.539 and 1.487 ms, respectively, corresponding (in accord with thermogravimetry) to $n = 0$.[35]

To show that these materials have potential applications in sensor devices, ITQMOF-1-Eu has been used to sense ethanol in air. This was done by monitoring the emission at 619 nm under an air stream alternatively saturated and not saturated with ethanol. Figure 4 shows a rapid decrease of the emission intensity in the presence of ethanol and a rapid recovery, almost to the initial value, when the sample is exposed to air. This behavior may be rationalized by considering that ethanol may coordinate to the Ln^{3+} ions, thus quenching the emission through coupling with the vibrational states of the O–H oscillators.[36] Similar results were obtained when the sample was exposed to a gaseous mixture containing water and ethanol, thus confirming the interest of the hydrophobic properties of the materials.

It is very important to mention that by careful choice of the Ln^{3+} ions it is possible to obtain materials with different emission (color) and magnetic properties (see the Supporting Information, Figure S11). For example, ITQMOF-1-Tb presents a ferromagnetic interaction between the Tb^{3+} ions and a strong green emission in UV light. At the same time, the ITQMOF-1-(5Eu-95Gd) sample shows an antiferromagnetic interaction between the Gd^{3+} ions and a red color in UV light, owing to the Eu ions.

Herein, we show that the judicious choice of an appropriate ligand (HFIPBB) allowed the design of novel lanthanide-based metal–organic frameworks with interesting multifunctional proper-

Table 1: Experimental $^5D_0$ lifetime, radiative (k_r) and nonradiative (k_{nr}) transition rates, $^5D_0$ quantum efficiency (q) and emission quantum yield (η, for excitation wavelengths 290 and 394 nm) of mixed Eu–Gd and pure Eu ITQMOF-1 single crystals.[a]

Sample	τ [ms]	k_r [s^{-1}]	k_{nr} [s^{-1}]	q [%]	η [%] (290 nm)	η [%] (394 nm)
ITQMOF-1-(5Eu-95Gd)	1.539 ± 0.006	535.6	113.8	83	48	13
ITQMOF-1-(66Eu-34Gd)	1.201 ± 0.004	575.4	257.6	69	45	32
ITQMOF-1-Eu	1.021 ± 0.041	551.2	428.4	56	36	28

[a] The data were obtained at room temperature and with the single crystals oriented horizontally relative to the detector.

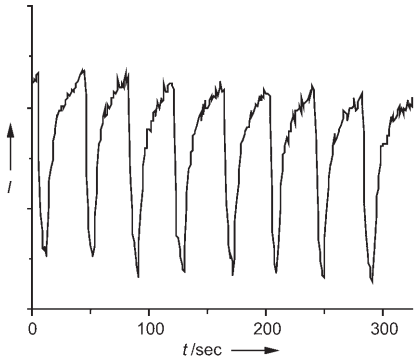

Figure 4. Test for sensing capabilities of the ITQMOF-1-Eu material. Variation of the fluorescence signal intensity at 619 nm under alternating streams of air saturated with ethanol (signal intensity decreases) and ethanol-free air (signal intensity increases).

ties (magnetism, luminescence, microporosity, and hydrophobicity) and high thermal stability. The combination of photoluminescent Ln^{3+} centers with the hydrophobic ligand HFIPBB resulted in materials which efficiently sense ethanol in the presence of water and under ambient conditions. Current studies are focused on exploring the combination of optical and magnetic properties of these materials for sensor applications and data storage.

Received: October 11, 2007
Published online: January 8, 2008

Keywords: lanthanides · luminescence · metal–organic frameworks · microporous materials · sensors

[1] C. C. Freyhardt, M. Tsapatsis, R. F. Lobo, K. J. Balkus, M. E. Davis, *Nature* **1996**, *381*, 295 – 298.
[2] A. Corma, M. J. Díaz-Cabanas, J. L. Jorda, C. Martínez, M. Moliner, *Nature* **2006**, *443*, 842 – 845.
[3] M. H. Kostova, D. Ananias, F. A. Almeida Paz, A. Ferreira, J. Rocha, L. D. Carlos, *J. Phys. Chem. B* **2007**, *111*, 3576 – 3582.
[4] B. D. Chandler, D. T. Cramb, G. K. H. Shimizu, *J. Am. Chem. Soc.* **2006**, *128*, 10403 – 10412.
[5] S. Surblé, C. Serre, F. Millange, F. Pellé, G. Férey, *Solid State Sci.* **2005**, *7*, 1074 – 1082.
[6] B. Chen, Y. Yang, F. Zapata, G. Lin, G. Qian, E. B. Lobkovsky, *Adv. Mater.* **2007**, *19*, 1693 – 1696.
[7] K. Kuriki, Y. Koike, Y. Okamoto, *Chem. Rev.* **2002**, *102*, 2347 – 2356.
[8] J.-L. Adam, *Chem. Rev.* **2002**, *102*, 2461 – 2476.
[9] J. Shi, W. Xu, Q. Li, F. Liu, Z. Huang, H. Lei, W. Yu, Q. Fang, *Chem. Commun.* **2002**, 756 – 757.
[10] T. Jüstel, H. Nikol, C. Ronda, *Angew. Chem.* **1998**, *110*, 3250 – 3271; *Angew. Chem. Int. Ed.* **1998**, *37*, 3084 – 3103.
[11] C. Seward, N.-X. Hu, S. Wang, *J. Chem. Soc. Dalton Trans.* **2001**, 134 – 136.
[12] T. Devic, C. Serre, N. Audebrand, J. Marrot, G. Férey, *J. Am. Chem. Soc.* **2005**, *127*, 12788 – 12789.
[13] X. Guo, G. Zhu, Z. Li, Y. Chen, X. Li, S. Qiu, *Inorg. Chem.* **2006**, *45*, 4065 – 4070.
[14] X. Guo, G. Zhu, Q. Fang, M. Xue, G. Tian, J. Sun, X. Li, S. Qiu, *Inorg. Chem.* **2005**, *44*, 3850 – 3855.
[15] J. Jia, X. Lin, A. J. Blake, N. R. Champness, P. Hubberstey, L. Shao, G. Walker, C. Wilson, M. Schröder, *Inorg. Chem.* **2006**, *45*, 8838 – 8840.
[16] N. L. Rosi, J. Kim, M. Eddaoudi, B. Chen, M. O'Keeffe, O. M. Yaghi, *J. Am. Chem. Soc.* **2005**, *127*, 1504 – 1518.
[17] F. Millange, C. Serre, J. Marrot, N. Gardant, F. Pellé, G. Férey, *J. Mater. Chem.* **2004**, *14*, 642 – 645.
[18] T. M. Reineke, M. Eddaoudi, M. Fehr, D. O. Kelley, M. Yaghi, *J. Am. Chem. Soc.* **1999**, *121*, 1651 – 1657.
[19] Y. J. Kim, M. Suh, D.-Y. Jung, *Inorg. Chem.* **2004**, *43*, 245 – 250.
[20] R.-G. Xiong, J. Zhang, Z.-F. Chen, X.-Z. You, C.-M. Che, H.-K. Fun, *J. Chem. Soc. Dalton Trans.* **2001**, 780 – 782.
[21] C. Serre, F. Millange, C. Thouvenot, N. Gardant, F. Pellé, G. Férey, *J. Mater. Chem.* **2004**, *14*, 1540 – 1543.
[22] T. K. Maji, G. Mostafa, H.-C. Chang, S. Kitagawa, *Chem. Commun.* **2005**, 2436 – 2438.
[23] J. N. Demas, B. A. DeGraff, P. B. Coleman, *Anal. Chem.* **1999**, *71*, 793A – 800A.
[24] J.-Y. Wu, T.-T. Yeh, Y.-S. Wen, J. Twu, K.-L. Lu, *Cryst. Growth Des.* **2006**, *6*, 467 – 473.
[25] T. Yuena, C. L. Lin, L. Pan, X. Huang, J. Li, *J. Appl. Phys.* **2006**, *99*, 08J501.
[26] A. Monge, N. Snejko, E. Gutierrez-Puebla, M. Medina, C. Cascales, C. Ruiz-Valero, M. Iglesias, B. Gomez-Lor, *Chem. Commun.* **2005**, 1291 – 1293.
[27] L. Pan, M. B. Sander, X. Huang, J. Li, M. Smith, E. Bittner, B. Bockrath, J. K. Johnson, *J. Am. Chem. Soc.* **2004**, *126*, 1308 – 1309.
[28] Crystal data for ITQMOF-1 $[Eu_2(C_{17}H_8F_6O_4)_3]$: $M_r = 1474.62$, hexagonal, tentative space group $P6/m$, $a = 21.379(9)$, $b = 21.379(9)$, $c = 7.073(6)$ Å, $V = 2799.5(2)$ Å^3, $Z = 2$, $\rho = 1.52\ g\,cm^{-3}$. Crystal data for ITQMOF-2 $[Eu_2(C_{17}H_8F_6O_4)_3]$ $M_r = 1474.62$, monoclinic, space group $P2_1/n$, $a = 7.2968(10)$, $b = 25.0695(10)$, $c = 29.4572(10)$ Å, $\beta = 91.920(5)°$, $V = 5385.5(8)$ Å^3, $Z = 4$, $\rho = 1.819\ g\,cm^{-3}$. CCDC 663383 (ITQMOF-2 material) contains the supplementary crystallographic data for this paper. These data can be obtained free of charge from The Cambridge Crystallographic Data Centre via www.ccdc.cam.ac.uk/data_request/cif.
[29] SHELXS-97—A program for automatic solution of crystal structures, G. M. Sheldrick, University of Goettingen, Germany, **1997**. Release 97 – 2.
[30] SHELXL-97—A program for crystal structure refinement. G. M. Sheldrick, University of Goettingen, Germany, **1997**. Release 97 – 2.
[31] O. L. Malta, M. A. Couto dos Santos, L. C. Thompson, N. K. Ito, *J. Lumin.* **1996**, *69*, 77 – 84.
[32] O. L. Malta, H. F. Brito, J. F. S. Menezes, F. R. Goncalves e Silva, S. Alves, Jr., F. S. Farias, Jr., A. V. M. de Andrade, *J. Lumin.* **1997**, *75*, 255 – 268.
[33] L. D. Carlos, Y. Messaddeq, H. F. Brito, R. A. Sa Ferreira, V. de Zea Bermundez, S. J. L. Ribeiro, *Adv. Mater.* **2000**, *12*, 594 – 598.
[34] M. F. Hazenkamp, G. Blasse, *Chem. Mater.* **1990**, *2*, 105 – 110.
[35] P. P. Barthelemy, G. R. Choppin, *Inorg. Chem.* **1989**, *28*, 3354 – 3357.
[36] N. Sabbatini, M. Guardigli, J.-M. Lehn, *Coord. Chem. Rev.* **1993**, *123*, 201 – 228.

